# A short note on accurate finite-difference modeling of anisotropic wave propagation

*Erik H. Saenger*

**email:** *saenger@geophysik.fu-berlin.de*
**keywords:** *rotated staggered finite-difference grid, anisotropic wave propagation*

## INTRODUCTION

Numerical modeling of seismic wave propagation in realistic (complex) media is an important tool used in earthquake and exploration seismology. It has been used to support interpretations of field data, to provide synthetic data for testing processing techniques and acquisition parameters, and to improve seismologists' understanding of seismic wave propagation. Since the widely used finite-difference (FD) approaches are based on the wave equation without physical approximations, the methods account not only for direct waves, primary reflected waves, and multiply reflected waves, but also for surface waves, head waves, converted reflected waves, and waves observed in ray-theoretical shadow zones (Kelly et al., 1976).

Staggered grid FD operators are commonly applied to compute the derivatives occurring in the wave equations for elastic, viscoelastic, and anisotropic media (e.g. (Virieux, 1986; Levander, 1988; Robertsson et al., 1994; Igel et al., 1995)). However, the standard FD operators cause instabilities when the medium possesses high contrasts in material properties. Boundary conditions of the elastic wavefield at high contrast discontinuities have to be defined explicitly in the FD algorithm (e.g. (Robertsson, 1996)). Instability problems can be avoided by using the so-called rotated staggered grid (RSG) technique (Saenger et al., 2000): the boundary conditions at high contrast discontinuities are implicitly fulfilled by the distribution of material parameters.

The numerical accuracy of the RSG for modeling scattering at empty fractures was successfully verified by comparison with an analytical solution (Krüger et al., 2002). Therefore, this grid is for example a powerful tool to study effective velocities in fractured media (Saenger and Shapiro, 2002; Saenger et al., 2002).

The RSG has been so far applied to displacement-stress formulations of the wave equations (Saenger et al. 2000). The first objective of this paper is to show that the RSG technique can also be adopted to velocity-stress formulations of the wave equations. Velocity-stress formulations are advantageous to model seismic wave absorption (Carcione et al., 1988; Robertsson et al., 1994; Bohlen, 2002). By applying the RSG to the 3-D viscoelastic wave equation it becomes possible to simulate the propagation of seismic waves in a viscoelastic medium containing voids or free surface topography without applying explicit boundary conditions.

The second objective of this paper is the application of the RSG-technique to the anisotropic elastic wave equation. Many papers (e.g. (Komatitsch et al., 2000; Carcione et al., 2002)) report that there is a disadvantage in using standard staggered grids for anisotropic media of symmetry lower than orthorhombic. Standard staggering implies that off-diagonal stress and strain components are not defined at the same location. When evaluating the stress-strain relation, it is necessary to sum over a linear combination of the elastic constants multiplied by the strain components. Hence some terms of the stress components have to be interpolated to the locations where the diagonal components are defined. This fact leads to an additional error in the dispersion analysis (Igel et al., 1995). For the rotated staggered grid such an interpolation is not necessary. We show with an accuracy analysis that the RSG can be advantageous for modeling general anisotropic media. The modeling of anisotropic elastic waves using the RSG is demonstrated with a simulation example.
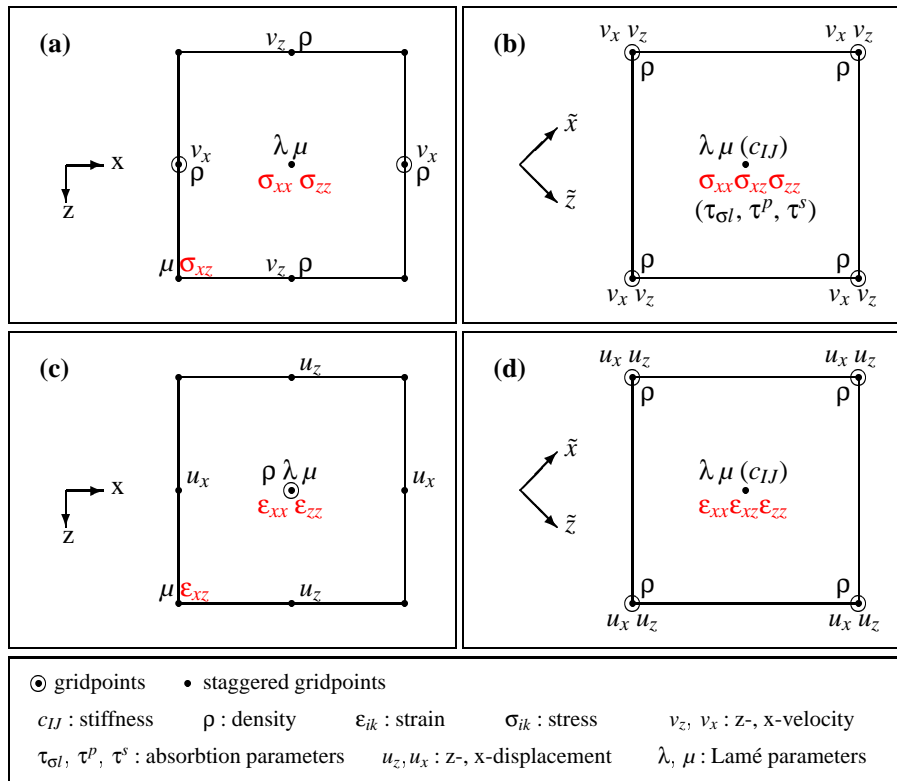
**Figure 1:** Elementary cells of different staggered grids. Locations where strains, displacements, velocities and elastic parameters are defined. **(a)** velocity-stress FD technique using a standard staggered grid. **(b)** velocity-stress FD technique using the rotated staggered grid. **(c)** displacement-stress FD technique using a standard staggered grid. **(d)** displacement-stress FD technique using the rotated staggered grid. Please note that for the RSG all components of one physical property are placed only at one location ((**b**) and (**d**)). This fact is the main reason for the enhanced (high-contrast) stability.

## THE PRINCIPLE OF THE ROTATED STAGGERED GRID: DISCRETIZATION

The differential equations and the basic numerical procedures for displacement-stress and velocity-stress FD schemes are well known and can be found in the papers mentioned above. Viscoelasticity can be implemented in velocity-stress schemes in a very efficient way. The parameters $\tau_{\sigma l}$, $\tau^p$ and $\tau^s$ can be optimized for the desired frequency independent Q (Blanch et al., 1995; Bohlen, 2002). The differential equations for the velocity-stress and the displacement-stress FD scheme were recast into discretized equivalents using staggered-grid approaches. As a result all modeling parameters are distributed at different (staggered and non-staggered) positions within the FD grid. The main idea of the rotated staggered grid is to change the directions of the derivatives to obtain a new distribution of modeling parameters. The necessary FD operators for the rotated and the standard staggered grid are discussed in detail in (Saenger et al., 2000).

For the sake of simplicity, we consider here an isotropic elastic medium in two dimensions with equal grid spacing in **z**- and **x**-direction. However, the results shown in Fig. 1 are also transferable to rectangular cells in three dimensions and all kinds of anisotropic elastic media.

The most important point is that for the RSG all components of one physical property are placed only at one single location (Fig. 1(b) and (d)). This fact is e.g. the main reason for the enhanced (high-contrast) stability. For the viscoelastic case in Fig. 1(b) the parameters $\tau_{\sigma l}$, $\tau^p$ and $\tau^s$ have the same position as $\sigma_{ij}$. For the rotated staggered grid in the case of anisotropic elastic media all elements of the elastic stiffness tensor $c_{ij}$ have the same position as for the isotropic case $\lambda$ and $\mu$ (see Fig. 1(b) and (d)). Therefore, the new distribution of elastic parameters is also advantageous for modeling in general anisotropic media, because no interpolation is necessary to calculate the Hook sum in the modeling algorithm.

## NUMERICAL STABILITY AND DISPERSION

In Saenger et al. (2000) numerical stability and grid dispersion of the RSG for isotropic elastic media are investigated. Though only the displacement-stress scheme is explicitly treated in this paper, all results also apply to the velocity-stress scheme (see also Moczo et al. (2000)). This can be reviewed by taking the difference of the finite-difference solution for the velocity components of the velocity-stress scheme at times $l + 1$ and $l$ and substituting the constitutive laws into the equation of motion. This provides a second-order system of difference equations in velocities only (Eq.(5) of Levander (1988)). The analogous equation of displacement-stress schemes for the derivation of the dispersion relation is Eq.(34) of Saenger et al. (2000). In this paper we extend the dispersion relation found by Igel et al. (1995) for general anisotropic 3D media using a $O(\Delta t^{N_{time}}, \Delta x^{N_{space}})$ standard staggered grid to the rotated staggered grid. As for the isotropic case the results are valid for displacement-stress and velocity-stress FD schemes. A general recipe how to extend the elastic dispersion analysis to the viscoelastic case can be found in Robertsson et al. (1994).

The general dispersion equation for the RSG and the standard staggered grid FD scheme express the frequency $\tilde{\omega}$ as a function of the numerical wavenumber $\tilde{\mathbf{k}}$, the eigenvalues $\lambda_l(\tilde{\mathbf{k}}, c_{IJ}, \rho, d_{\underset{ij}{\rightarrow}}, d_{\underset{ji}{\leftarrow}})$ of the matrix $\underline{\hat{\mathbf{M}}}$ ($l = 1, 2, 3$ for qP-, qS1- and qS2-waves), and the order of the time extrapolation $N_{time}$ as (Eq.(45) of Igel et al. (1995)):

$$\tilde{\omega}_l(\mathbf{k}, \Delta t) = \frac{2}{\Delta t} \arcsin \sqrt{-\frac{1}{2} \sum_{n=1}^{N_{time}/2} (-1)^n \lambda_l^n(\tilde{\mathbf{k}}, c_{IJ}, \rho, d_{\underset{ij}{\rightarrow}}, d_{\underset{ji}{\leftarrow}}) \frac{\Delta t^{2n}}{(2n)!}}, \tag{1}$$

where $\Delta t$ is the time increment of the used FD scheme, $c_{IJ}$ are the elements of the elastic stiffness tensor, $\rho$ denotes the density, and $d_{\underset{ij}{\rightarrow}}$, $d_{\underset{ji}{\leftarrow}}$ are interpolation operators. The definition of the matrix $\underline{\hat{\mathbf{M}}}$ is given with Eq.(44) of Igel et al. (1995).

For the standard staggered grid one has to use (in Eq.(1)) the following numerical wavenumber $\tilde{k}_j$ and the interpolation operators $d_{\underset{ij}{\rightarrow}}$ and $d_{\underset{ji}{\leftarrow}}$:

$$\tilde{k}_j = \frac{2}{\Delta x_j} \sum_{m=1}^{N_{space}/2} \left[ p_m \sin(k_j \frac{2m-1}{2} \Delta x_j) \right] \tag{2}$$

(Eq.(5) of Crase (1990) and Eq.(35) of Igel et al. (1995)),

$$d_{\underset{ij}{\rightarrow}} = d_{\underset{ji}{\leftarrow}} = 2 \sum_{m=1}^{N_{space}/2} \left[ d_m \cos(k_i \frac{2m-1}{2} \Delta x_i) \cos(k_j \frac{2m-1}{2} \Delta x_j) \right] \tag{3}$$

(Eq.(22) of Igel et al. (1995) and text below), where $\Delta x_j$ is the grid spacing in the $j$-direction, $k_j$ is the $j$th component of the wavenumber $\mathbf{k}$, $p_m$ are the finite-difference coefficients (e.g. (Holberg, 1987)) and $d_m$ are the coefficients of the interpolation operator.

For the rotated staggered grid one has to use (in Eq.(1)) the numerical wavenumber $\tilde{k}_j^{rot}$. The interpolation operators $d_{\underset{ij}{\rightarrow}}^{rot}$ and $d_{\underset{ji}{\leftarrow}}^{rot}$ are simply equal one because this kind of interpolation is not necessary for the RSG:

$$\tilde{k}_j^{rot} = \frac{2}{\Delta x_j} \sum_{m=1}^{N_{space}/2} \left[ p_m \sin(k_j \frac{2m-1}{2} \Delta x_j) \prod_{\substack{i=1 \\ i \neq j}}^{3} \cos(k_i \frac{2m-1}{2} \Delta x_i) \right], \tag{4}$$

$$d_{\underset{ij}{\rightarrow}}^{rot} = d_{\underset{ji}{\leftarrow}}^{rot} = 1. \tag{5}$$

The stability criterion for a $O(\Delta t^{N_{time}}, \Delta x^{N_{space}})$ FD scheme can be found by analyzing the following inequality (Crase, 1990):

$$0 \leq -\frac{1}{2} \sum_{n=1}^{N_{time}/2} (-1)^n \lambda_l^n(\tilde{\mathbf{k}}, c_{IJ}, \rho, d_{\underset{ij}{\rightarrow}}, d_{\underset{ji}{\leftarrow}}) \frac{\Delta t^{2n}}{(2n)!} \leq 1 \tag{6}$$
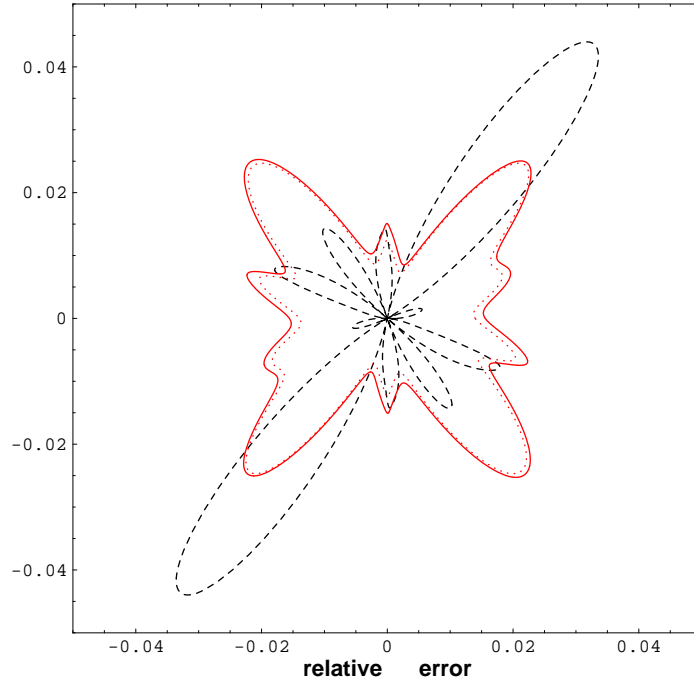
**Figure 2:** A comparison of the relative error of the phase velocity ($A_{rel} = |\omega(\mathbf{k})/(v_{ph}(\mathbf{k})|\mathbf{k}|) - 1|$) of the qS2-wave in the xz-plane between the standard staggered grid and the rotated staggered grid is shown. The medium has triclinic symmetry. The dashed line represents the results for the standard staggered grid, and the solid line shows the results for the rotated staggered grid with exactly the same modeling parameters. The dotted line is obtained for the rotated staggered grid with an increased timestep by a factor of $\sqrt{3}$ (The RSG is in general more stable than the standard staggered grid).

For a general anisotropic medium this is not easily calculated. However, the stability criterion for velocity-stress and displacement-stress RSG schemes (2nd order time, i.e. $N_{time} = 2$) for isotropic media can be found in Saenger et al. (2000):

$$\frac{\Delta t v_p}{\Delta h} \leq 1/(\sum_{k=1}^{N_{space}} |p_k|). \tag{7}$$

In this equation $v_p$ denotes the compressional wave velocity and $\Delta h$ the grid spacing. For the 3D case this is more stable by a factor of $\sqrt{3}$ than for the standard staggered grid (Saenger et al., 2000). In the anisotropic case, a good first approximation can be made by replacing $v_p$ in Eq.(7) by the maximum phase velocity of the anisotropic media (Igel et al., 1995).

For a comparison of both finite-difference schemes (i.e. the RSG and the standard staggered grid) we consider exactly the same triclinic media as defined in Eq.(47) of Igel et al. (1995). We focus on the qS2-wave case because there one can observe the maximum relative error of the phase velocity (see e.g. Fig. 6 of Igel et al. (1995)). Here we compare both schemes with a relative accuracy of $O(\Delta t^2, \Delta x^2)$ at 20% Nyquist (dispersion parameter $H = |\mathbf{k}|\Delta h/(2\pi) = 0.1$) with $\Delta t = 0.146(s/m)\Delta x$. This is about 20% of the stability limit for the standard staggered grid. The used coefficients of the FD and the interpolation operators are $p_1 = 1$ and $d_1 = 0.5$, respectively. The results in Fig. 3 can qualitatively compared with the qS2-case of Fig. 7 of Igel et al. (1995). The conclusion of our dispersion analysis between the two different FD schemes is obvious: For this specific triclinic medium the application of the rotated staggered grid is advantageous. However, for any triclinic medium one has to repeat the analysis described above because:

- The error of the wave properties in the general anisotropic case for staggered finite difference grids depends on the length of the used operators, the symmetry system of the anisotropic medium, the orientation of the symmetry axis with respect to the coordinate axis and, this is very important, the degree of anisotropy (Igel et al., 1995).

- The ratio of the maximum relative error of the phase velocity between the RSG and the standard staggered grid depends for general anisotropic media on the dispersion parameter $H = |\mathbf{k}|\Delta h/(2\pi)$.

## ANISOTROPIC MODELING EXAMPLE

The RSG has been applied to a displacement-stress formulation of the 2D elastic wave equation for anisotropic media. In the example we demonstrate that the RSG allows for modeling anisotropic wave propagation in media with a strong contrast in elastic parameters. We built a 2D-model with two different half-spaces surrounded by a thin ($0.5cm$) vacuum layer ($c_{IJ} = 0$, $\rho = 0.00001 kg/m^3$). The two half-spaces have a total size of $68cm \times 64cm$ using a grid spacing of $0.5mm$. The left-hand side is a transversely isotropic zinc crystal which is characterized by $c_{11} = 16.5 \times 10^{10}\ N/m^2$, $c_{13} = 5 \times 10^{10}\ N/m^2$, $c_{33} = 6.2 \times 10^{10}\ N/m^2$, $c_{55} = 3.96 \times 10^{10}\ N/m^2$ and a density of $\rho = 7100\ kg/m^3$. For the isotropic media (an 'isotropic' version of zinc) on the right-hand side we use $c_{11} = 16.5 \times 10^{10}\ N/m^2$, $c_{55} = 3.96 \times 10^{10}\ N/m^2$ and $\rho = 7100 kg/m^3$. The source is a vertical point force (with a Gaussian taper) located $2cm$ to the left of the interface in the anisotropic half-space. The source time function is a Ricker wavelet with dominant frequency $f_0 = 170 KHz$. The simulation uses 4000 timesteps of $\Delta t = 25ns$. To interpret the different phases in the first snapshot shown in Fig. 3 we refer to Carcione et al. (1992) and Komatitsch et al. (2000). They have studied previously a (very) similar problem.
As mentioned by Hestholm (2002) high-order FD methods will not decrease the numerical dispersion of Rg (fundamental mode Rayleigh) waves, only closer spatial sampling will, so second-order FDs may as well be used along a free surface topography. Consequently, below the vacuum (the three 'free' surfaces of our model), the FD order is gradually increased via 4 and 6 up to 8, which is the order in the interior of the medium. In the second snapshot of the simulation (Fig. 3) the interaction of the different waves with the 'free' surfaces is shown.

## CONCLUSIONS

We have shown that the rotated staggered grid can be applied to the velocity-stress formulation of the viscoelastic wave equation and to the displacement-stress formulation of the elastic wave equation for anisotropic media. In both cases implementation of the RSG expands the range of applications. The new FD algorithm allows modeling of absorbing media with high contrast in material properties. Additionally, wave propagation in 3D anisotropic media can be modeled very accurately, because in contrast to standard staggered grid schemes no interpolation is necessary to calculate the Hook sum. The method is efficient and flexible and has a broad range of practical use, for example modeling of small-scale cracks (e.g. filled with viscous fluid) or topography of the earth surface.

## ACKNOWLEDGEMENTS

## REFERENCES

Blanch, J. O., Robertsson, J. O. A., and Symes, W. W. (1995). Modeling of a constant Q: Methodology and algorithm for an efficient and optimally inexpensive viscoelastic technique. *Geophysics*, 60:176–184.

Bohlen, T. (2002). Parallel 3-D viscoelastic finite difference seismic modeling. *Computers and Geosciences*, 28:887–899.

Carcione, J. M., Herman, G. C., and ten Kroode, A. P. E. (2002). Seismic modeling. *Geophysics*, 67:1304–1325.
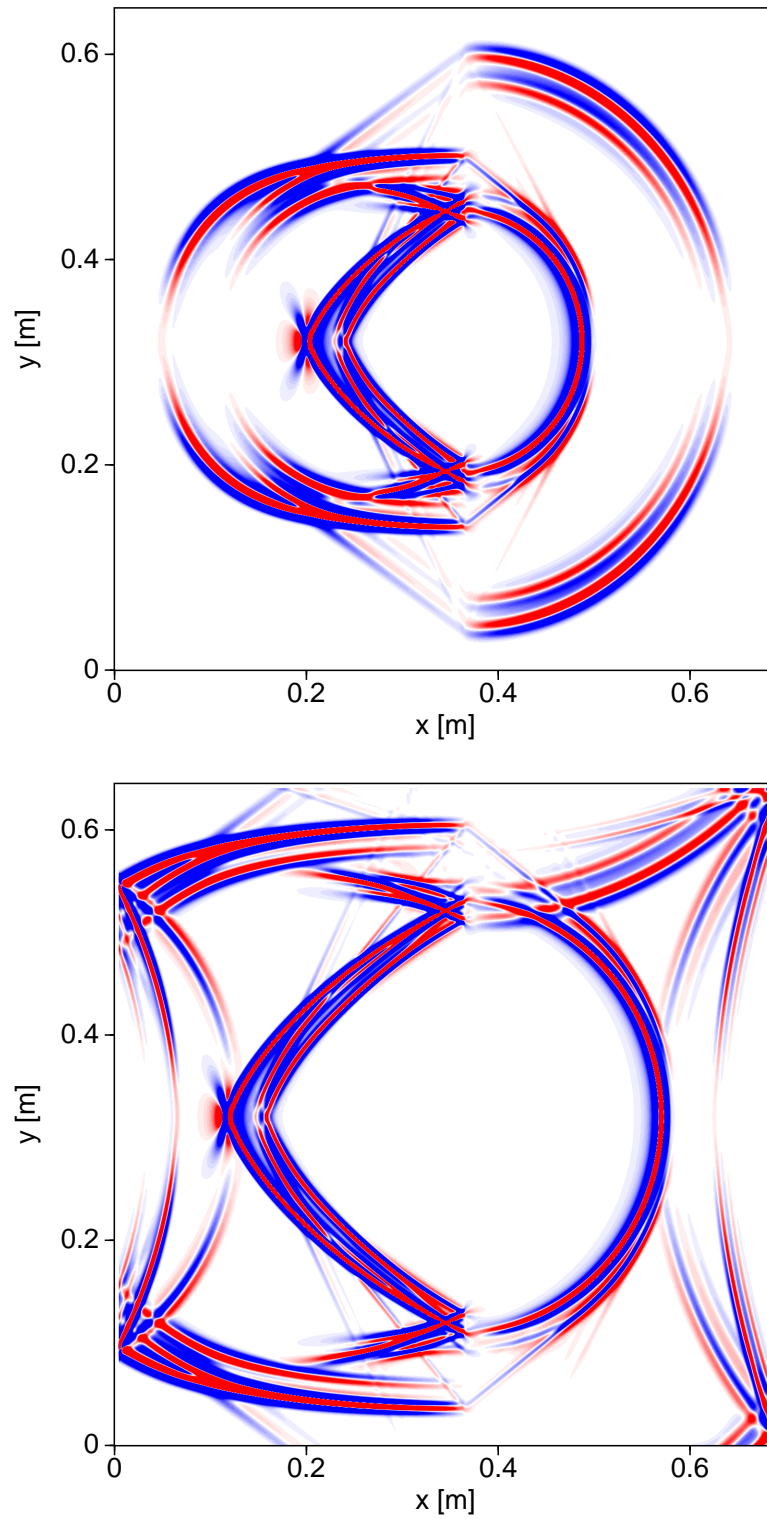
**Figure 3:** Two snapshots (vertical displacement) of an anisotropic FD experiment using the rotated staggered grid at two different timesteps. The model is composed of two half-spaces: a transversely isotropic zinc crystal with vertical symmetry axis on the left, and an isotropic material on the right. The two halfspaces are surrounded at three sides by a thin vacuum layer. A similar problem was previously studied by Carcione et al. (1992) and Komatitsch et al. (2000).

Carcione, J. M., Kosloff, D., Behle, A., and Seriani, G. (1992). A spectral scheme for wave propagation simulation in 3-D elastic-anisotropic media. *Geophysics*, 57:1593–1607.

Carcione, J. M., Kosloff, D., and Kosloff, R. (1988). Viscoacoustic wave propagation simulation in the earth. *Geophysics*, 53:769–777.

Crase, E. (1990). High-order (space and time) finite-difference modeling of the elastic wave equation. In *60th Annual Internat. Mtg., Soc. Expl. Geophys., Expanded Abstracts*, volume 90, pages 987–991.

Hestholm, S. (2002). Composite memory variable velocity-stress viscoelastic modelling. *Geophys. J. Int.*, 148:153–162.

Holberg, O. (1987). Computational aspects of the choice of operator and sampling interval for numerical differentiation in large-scale simulation of wave phenomena. *Geophysical Prospecting*, 35:629–655.

Igel, H., Mora, P., and Riollet, B. (1995). Anisotropic wave propagation through finite-difference grids. *Geophysics*, 60:1203–1216.

Kelly, K. R., Ward, R. W., Treitel, S., and Alford, R. M. (1976). Synthetic seismograms: A finite-difference approach. *Geophysics*, 41:2–27.

Komatitsch, D., Barnes, C., and Tromp, J. (2000). Simulation of anisotropic wave propogation based upon a spectral element method. *Geophysics*, 65(4):1251–1260.

Krüger, O. S., Saenger, E. H., and Shapiro, S. (2002). *Simulation of the diffraction by single cracks: an accuracy study*, page SM P1.2. 72st Ann. Internat. Mtg, Soc. of Expl. Geophys.

Levander, A. R. (1988). Fourth-order finite-difference P-SV seismograms. *Geophysics*, 53:1425–1436.

Moczo, P., Kristek, J., and Halada, L. (2000). 3D 4th-order staggered-grid finite-difference schemes: Stability and grid dispersion. *Bulletin of the Seismological Society of America*, 90:587–603.

Robertsson, J. A., Blanch, J. O., and Symes, W. W. (1994). Viscoelastic finite difference modeling. *Geophysics*, 59:1444–1456.

Robertsson, J. O. A. (1996). A numerical free-surface condition for elastic/viscoelastic finite-difference modeling in the presence of topography. *Geophysics*, 61:1921–1934.

Saenger, E. H., Gold, N., and Shapiro, S. A. (2000). Modeling the propagation of elastic waves using a modified finite-difference grid. *Wave Motion*, 31(1):77–92.

Saenger, E. H., Krüger, O. S., and Shapiro, S. (2002). *Simulation of effective elastic properties of 3D fractured medium*, page RP 1.3. Soc. of Expl. Geophys.

Saenger, E. H. and Shapiro, S. A. (2002). Effective velocities in fractured media: A numerical study using the rotated staggered finite-difference grid. *Geophysical Prospecting*, 50(2):183–194.

Virieux, J. (1986). Velocity-stress finite-difference method. *Geophysics*, 51:889–901.